NASA TECHNICAL NOTE

NASA TN D-4062

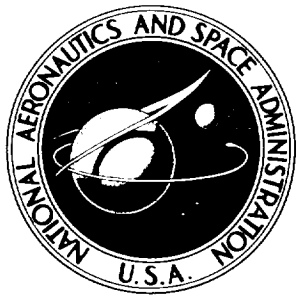

NASA TN D-4062

FULL-SCALE INVESTIGATION OF THE AERODYNAMIC CHARACTERISTICS OF A MODEL EMPLOYING A SAILWING CONCEPT

by Marvin P. Fink

Langley Research Center
Langley Station, Hampton, Va.

NATIONAL AERONAUTICS AND SPACE ADMINISTRATION • WASHINGTON, D. C. • JULY 1967

NASA TN D-4062

FULL-SCALE INVESTIGATION OF THE AERODYNAMIC CHARACTERISTICS OF A MODEL EMPLOYING A SAILWING CONCEPT

By Marvin P. Fink

Langley Research Center
Langley Station, Hampton, Va.

NATIONAL AERONAUTICS AND SPACE ADMINISTRATION

For sale by the Clearinghouse for Federal Scientific and Technical Information
Springfield, Virginia 22151 – CFSTI price $3.00

FULL-SCALE INVESTIGATION OF THE AERODYNAMIC CHARACTERISTICS OF A MODEL EMPLOYING A SAILWING CONCEPT

By Marvin P. Fink
Langley Research Center

SUMMARY

An investigation has been conducted in the Langley full-scale tunnel to determine the aerodynamic characteristics of a full-scale model employing a sailwing concept and having a wing aspect ratio of 11.5. The wing had a rigid leading-edge spar, rigid root and wing-tip ribs, with a trailing-edge cable stretched between these ribs, and a fabric covering stretched between the leading and trailing edges.

The fabric of the sail maintained a smooth airfoil contour over the unstalled angle-of-attack range, but some rippling occurred at the trailing edge near the wing root as the wing stalled. The aerodynamic characteristics of the sailwing, in particular the maximum lift and maximum lift-drag ratio, compared favorably with those of conventional hard wings. A lateral-control device based on the wing-warp principle was effective at angles of attack below that for wing stall, but at angles near stall, the control effectiveness became low and nonlinear.

INTRODUCTION

There have been many schemes in which the conventional rigid type of construction of an airplane wing was replaced with a minimum-structure fabric surface in an effort to achieve structural simplicity. One such device, first conceived as an advanced sail for a boat, was later converted to an airplane wing. This type of wing uses a single spar as the wing leading edge and main load-carrying member, ribs only at the wing tips and root, a wire trailing edge stretched between these ribs, and a fabric envelope to form the wing surface. A device of this type, called a sailwing (devised at Princeton University), has been tested in the Langley full-scale tunnel to evaluate the aerodynamic characteristics of a wing of this simplified type of structure.

The model used in the investigation was a full-scale airplane with a wing having an aspect ratio of 11.5. The investigation was made to determine the lift, drag, and static-stability characteristics, and lateral control effectiveness.

SYMBOLS

Figure 1 shows the stability-axis system used in the presentation of the data and the positive directions of the forces, moments, and angles. The data are computed about the moment center shown in figure 2(a). Measurements for this investigation were taken in the U.S. Customary System of Units. Equivalent values are indicated herein in the International System of Units (SI) in the interest of promoting the use of this system in future NASA reports. Details concerning the use of SI, together with physical constants and conversion factors, are given in the appendix and in reference 1.

C_D drag coefficient, $\frac{\text{Drag}}{qS}$

C_D' drag coefficient about stability axis

C_L lift coefficient, $\frac{\text{Lift}}{qS}$

C_l rolling-moment coefficient, $\frac{\text{Rolling moment}}{qSb}$

C_m pitching-moment coefficient, $\frac{\text{Pitching moment}}{qS\bar{c}}$

C_n yawing-moment coefficient, $\frac{\text{Yawing moment}}{qSb}$

C_Y side-force coefficient, $\frac{\text{Side force}}{qS}$

$C_{l_\beta} = \frac{\partial C_l}{\partial \beta}$

$C_{n_\beta} = \frac{\partial C_n}{\partial \beta}$

$C_{Y_\beta} = \frac{\partial C_Y}{\partial \beta}$

A aspect ratio

b wing span, 30.5 ft (9.30 meters)

$C_{m_{\delta_e}}$ elevator-control power parameter

$\bar{c}$ mean aerodynamic chord, 2.59 ft (0.79 meter)

$\frac{c_a}{c}$	ratio of aileron chord length to wing chord length
L/D	lift-drag ratio
$\frac{pb}{2V}$	roll-rate parameter
q	free-stream dynamic pressure, $\frac{\rho V^2}{2}$, lb/ft^2 (newtons/meter^2)
R	Reynolds number, $\frac{\rho V \bar{c}}{\mu}$
S	wing area, 81.5 ft^2 (7.57 meter^2)
V	free-stream velocity, ft/sec (meters/second)
x,y,z	distances along X-, Y-, and Z-axes, in. (cm)
$\frac{y}{b/2}$	ratio of lateral distance from center line of model to model semispan
α	angle of attack of fuselage reference line, deg (see fig. 2)
β	sideslip angle, deg
δ_a	total wing-tip-control deflection, deg
$\delta_{a,L}$	left wing-tip deflection for roll control, positive with trailing edge down, deg
δ_e	elevator deflection, positive with trailing edge down, deg
λ	taper ratio
μ	coefficient of viscosity
ρ	mass density of air, slugs/ft^3 (kilogram/meter^3)

MODEL AND TESTS

Model

The configuration tested in the current investigation was a full-scale airplane model. Figure 3 presents a photograph of the model mounted in the tunnel test section. A three-view drawing showing the general arrangement of the model and the principal dimensions is given in figure 2(a). The wing had an aspect ratio of 11.5 and a taper ratio of 0.4. Figure 2(b) shows a typical cross section of the wing. The wing construction consisted of a D-spar leading edge drooped 8°, a wire trailing edge, and rigid ribs at the wing tips and root. This framework was covered with a fabric envelope which formed the upper and lower surfaces of the wing. The fabric was stretched taut by adjustable tension bridle wires attached to the trailing edge as shown in figure 2(a). The model was laterally controlled by means of hinged wing tips which effectively caused wing warping. The controls were constructed so that the projection of the hinge line of the movable-wing-tip rib extended from the hinge located on the wing spar at the tip of the wing to the trailing edge of the wing root. (See fig. 2(a).) The left-wing-tip control was instrumented so that the control hinge moment could be measured.

Tests

Tests were made to determine the aerodynamic characteristics of the novel type of wing used on the model. The principal characteristics of interest were (1) lift and drag, (2) static longitudinal and lateral stability, and (3) lateral control. The tests were made in the Langley full-scale tunnel which is described in reference 2. The model was tested over an angle-of-attack range from about -8° to 20° for a range of tunnel velocity from about 38 ft/sec (11.6 m/sec) to about 85 ft/sec (25.9 m/sec) at sideslip angles of $\pm 5^{\circ}$. Tests were also made with the elevator deflected 20° and with the horizontal tail removed. Lateral-control effectiveness tests were made for a range of approximately $\pm 15^{\circ}$ of control deflection. The fuselage alone was tested over the angle-of-attack range at zero sideslip. The results have been corrected for airstream misalinement, strut tares, and tunnel-wall effects.

RESULTS AND DISCUSSION

Complete-Model Configuration

Longitudinal aerodynamic characteristics.- The longitudinal aerodynamic characteristics for the complete-airplane configuration are given in figure 4 for a range of tunnel dynamic pressure from 1.66 lb/ft^2 (79.5 N/m^2) to 6.83 lb/ft^2 (327.0 N/m^2). These data show that, in general, the aerodynamic characteristics of the wing were not appreciably affected by change in dynamic pressure except that the maximum lift and stall angle

increased slightly with increase in dynamic pressure. A study of the motion pictures taken during the tests revealed that the sail maintained essentially a smooth airfoil contour over the speed range except that at angles of attack near maximum lift some rippling occurred at the trailing edge near the wing root and indicated the presence of stall. A maximum lift coefficient of 1.54 was obtained at an angle of attack of about 15° at $q = 6.83$ lb/ft^2 (327.0 N/m^2). A maximum L/D of 12.9 for the complete-airplane configuration was reached at $\alpha = 3^{\circ}$ ($C_L = 1.08$) and $q = 2.72$ lb/ft^2 (130.2 N/m^2).

The effect of the bridle wires on the longitudinal aerodynamic characteristics is shown in figure 5. These data show that for angles of attack below about 10°, lift was reduced when some or all the bridle wires were removed; but for all other angles of attack maximum lift was higher. Removal of the bridle wires also caused a reduction in the maximum value of L/D. It appears, therefore, that the choice of the number of bridle wires used to restrain the trailing-edge deformation is a trade-off between maximum lift and maximum L/D.

The results of tail-off and elevator-effectiveness tests are presented in figure 6. These data, as well as the data of figures 4 and 5, show that the model was longitudinally stable over the entire angle-of-attack range including angles above that required for maximum lift. Only two elevator deflections, $\delta_e = 0^{\circ}$ and 20°, were tested, but these limited data indicate that the elevator was capable of trimming the airplane over the angle-of-attack range with a nearly constant value of control power $\left(C_{m_{\delta_e}} = -0.032 \text{ per degree}\right)$.

The results of tests to determine the effects of sideslip on the longitudinal aerodynamic characteristics of the complete model are shown in figure 7. These data show that there were no very significant effects of sideslip.

Lateral-stability characteristics.- The lateral-stability characteristics of the complete-model configuration are presented in figure 8 over an angle-of-attack range at $\pm 5^{\circ}$ of sideslip. These data are replotted in figure 9 to show the sideslip lateral-stability derivatives as determined from the forces and moments measured at $\pm 5^{\circ}$ sideslip. These sideslip derivatives show that the complete-model configuration was directionally stable over most of the angle-of-attack range. However, the stability was low, the value of C_{n_β} being about 0.0004 over most of the angle-of-attack range and nearly zero at angles of attack near stall. The model had positive dihedral effect $\left(-C_{l_\beta}\right)$ over the entire angle-of-attack range. At angles of attack near stall, the basic configuration showed very high lateral stability with an effective dihedral angle of about 16°.

Lateral-control characteristics.- The variations of the lateral-control characteristics with total control deflection are shown in figure 10. During these tests, the controls were moved by an actuator attached to the aileron-control bellcrank in the fuselage. Control-position indicators were attached to each tip control to indicate the individual control deflections. The right wing tip was set to a predetermined deflection, and the

left-wing-tip deflection was recorded. The controls were rigged for approximately a 1:1 ratio of up and down deflection, but because of control cable stretch the ratio was not always exact. Hence, the actual deflection of the right and left wing tips corresponding to the total deflection is given at the top of the figure on the abscissa scale. The data of figure 10 show that the lateral-control effectiveness is fairly linear for the two lower angles of attack, $\alpha = 1.0^{\circ}$ and 4.9°. These angles of attack correspond approximately to lift coefficients of 0.8 and 1.2, respectively. For the highest angle of attack, $\alpha = 14.9^{\circ}$, however, the control effectiveness was low and nonlinear. This angle of attack is approximately the angle of attack for the stall at a lift coefficient of about 1.4; therefore it is not surprising that the control effectiveness is not a linear function of deflection.

One point that should be made in connection with the lateral-control data is the probable effect of damping in roll on the rolling velocity resulting from lateral-control deflection. It may be noted from figure 4 that there is a marked reduction in lift-curve slope at angles of attack above about 2° or 3°; for example, the lift-curve slope at $\alpha = 4.9^{\circ}$ is only about 60 percent that at $\alpha = 1.0^{\circ}$. Since damping in roll is a function of lift-curve slope, it would be expected that the damping in roll would be correspondingly lower at the higher angle of attack. In this case the static-control effectiveness is not a definite indication of the effectiveness of the lateral control in producing a rolling velocity; and the airplane would be expected to roll faster in terms of the nondimensional roll rate parameter $\frac{pb}{2V}$ at $\alpha = 4.9^{\circ}$ than at $\alpha = 1.0^{\circ}$ even though the static-control effectiveness is about the same for the two conditions. (See fig. 10.)

In figure 11 a comparison is made of the rolling moment produced by total control deflection of the sailwing with that of a theoretical aileron having a value of aileron—wing-chord ratio of 0.15 and comprising the outboard 30 percent of the wing span of a wing having the same aspect ratio and taper ratio as the sailwing. It is shown in this figure that the wing-warp method of roll control used on the sailwing corresponds to that produced by a normal aileron of this size.

Wing-tip hinge moment.- Lateral-control hinge-moment data for the left wing tip were taken in conjunction with the data of figure 10 and are presented in figure 12 plotted against the left-wing-tip control deflection for several angles of attack. Two points are evident from inspection of these data. One point is that the hinge moment increased as the angle of attack, and consequently the lift, was increased. This characteristic results from the fact that an increase in lift causes an increase in the upload on the trailing-edge wire which is attached to the rear of the wing-tip rib. The second point is that the hinge-moment curves show increasing moment for increasing downward deflection, which is a stable variation, for the two lower angles of attack ($\alpha = 1.0^{\circ}$ and 4.9°) which are in the unstalled lift range. The data show the opposite, or unstable, slope for $\alpha = 14.6^{\circ}$ which is approximately the angle for maximum lift.

Wing-Alone Characteristics

Wing-alone characteristics were determined by subtracting measured aerodynamic characteristics of the fuselage from the characteristics of the complete model with the horizontal tail removed which are presented in figure 6. The longitudinal characteristics of the fuselage are presented in figure 13. These data were taken for the fuselage with the wings, horizontal tail, and all struts and bridle wires removed. The data presented for the wing alone, therefore, include the drag of the bridle wires, the struts, and the wing-fuselage interference. The wing-alone longitudinal aerodynamic characteristics determined by the foregoing procedure are shown in figure 14, and the profile drag and the lift-drag ratios for the wing alone are compared with those of conventional wind-tunnel models in figures 15 and 16.

Lift.- The data of figure 14 for $q \approx 3.26$ lb/ft (156.1 N/m^2) show that the lift characteristics for the wing alone are basically the same as those for the complete model. A maximum lift coefficient of 1.5 was obtained at an angle of attack of about 15°. The lift-curve slope changes markedly over the unstalled angle-of-attack range. The slope was unusually steep at low angles of attack (from -8° to -5°). In fact, the maximum lift-curve slope was 7.16 per radian (0.125 per degree) which is greater than the theoretical two-dimensional lift-curve slope of a rigid airfoil (2π). As the angle of attack was increased, for example, from 1° to 5°, the lift-curve slope is down to a normal value of 4.01 per radian (0.07 per degree). This characteristic of a steep lift curve at low lift coefficients and a much lower lift-curve slope at higher angles of attack results from the fact that the camber of the airfoil increases markedly with increase in angle of attack in the low lift range when the wing fabric and wires are not very taut. This increasing camber with increasing angle of attack results in an unusually high lift-curve slope. At high lift coefficients, however, the fabric and wires are taut and do not stretch much; therefore the camber does not change appreciably and the lift curve has the normal slope of a fixed airfoil.

Pitching moment.- The pitching-moment data of figure 14, which are referred to the $\bar{c}/4$ location, on the wing, indicate that the wing was longitudinally stable over the angle-of-attack range and the aerodynamic center was at about the $0.40\bar{c}$ station. This unusually rearward location of the aerodynamic center results from the aforementioned characteristics of the wing of changing camber as angle of attack increases.

Drag.- In the plot of C_D as a function of $C_L{}^2$ of figure 15, it may be noted that the wing has high profile drag, as compared with the conventional hard wing, in the low lift range. As the angle of attack is increased and the sail attains camber and tautness, the profile drag is about the same as that of a conventional wing of similar geometric characteristics. In fact, the drag of the sailwing is lower than that of the conventional wing at high lift coefficients where the sailwing has much higher camber than the hard

wing. A slope taken through the linear portion of the polar ($C_L{}^2$ from about 0.7 to 1.6) indicates a span-efficiency factor $C_L{}^2/\pi A$ of about 0.75 for the sailwing.

Lift-drag ratio.- Although an exact comparison of the sailwing with a wing of conventional construction is not intended in this report, figure 16 is presented to show the general relationship of the lift-drag ratios. Here, it may be noted that the sailwing reached a maximum value of L/D of about 28 which is about the same as that achieved with smooth conventional wind-tunnel models of approximately the same aspect ratio. (See refs. 3 and 4.) Because of the highly cambered airfoil section, the sailwing reached maximum L/D at a considerably higher lift coefficient than that for the hard wings.

CONCLUDING REMARKS

An experimental investigation to determine the aerodynamic characteristics of a full-scale model employing a sailwing concept has been made and the following conclusions were drawn from the results of this investigation:

1. The fabric of the sail maintained a smooth airfoil contour over the unstalled angle-of-attack range, but some rippling occurred at the trailing edge near the wing root as the wing stalled.

2. The sailwing attained a maximum value of lift-drag ratio comparable with those of similar conventional hard wings.

3. The lift curve had the characteristic of an unusually steep lift-curve slope (high C_{L_α}) at low angles of attack (from -8° to -5°) as the airfoil experienced a rapid increase in camber with increasing angle of attack. The lift-curve slope was more normal at high angles of attack when the wing fabric and rigging wires became taut; therefore, the airfoil did not change camber much with increasing angle of attack.

4. The aerodynamic center of the wing was unusually rearward, at about the 0.40 mean aerodynamic chord station, because of the wing characteristic of increasing camber with increasing lift.

5. The lateral-control device which provided roll control by the wing-warp technique was effective up to angles of attack near maximum lift where control effectiveness became low and nonlinear.

6. Sail tautness and trailing-edge deformation which is controlled primarily by the arrangement of the trailing-edge bridle wires had a noticeable effect on the aerodynamic characteristics.

Langley Research Center,
National Aeronautics and Space Administration,
Langley Station, Hampton, Va., March 20, 1967,
126-13-01-60-23.

APPENDIX

CONVERSION FACTORS – U.S. CUSTOMARY UNITS TO SI UNITS

The International System of Units (SI) was adopted by the Eleventh General Conference on Weights and Measures, Paris, October 1960. (See ref. 1.) The following conversion factors are included in this report for convenience:

Physical quantity	U.S. Customary Unit	Conversion factor (*)	SI Unit
Area	ft^2	0.0929	$meters^2$ ($m2$)
Density	$slugs/ft^3$	515.379	$kilograms/meter^3$ ($kg/m3$)
Force	lbf	4.44822	newtons (N)
Length	in.	0.0254	meters (m)
	ft	0.3048	meters (m)
Moment	lbf-ft	1.356	newton-meters (N-m)
Pressure	lbf/ft^2	47.88	$newtons/meter^2$ ($N/m2$)
Velocity	ft/sec	0.3048	meters/second (m/sec)

*Multiply value given in U.S. Customary Unit by conversion factor to obtain equivalent value in SI Unit.

REFERENCES

1. Mechtly, E. A.: The International System of Units – Physical Constants and Conversion Factors. NASA SP-7012, 1964.

2. DeFrance, Smith J.: The N.A.C.A. Full-Scale Wind Tunnel. NACA Rept. 459, 1933.

3. Neely, Robert H.; Bollech, Thomas V.; Westrick, Gertrude C.; and Graham, Robert R.: Experimental and Calculated Characteristics of Several NACA 44-Series Wings With Aspect Ratios of 8, 10, and 12 and Taper Ratios of 2.5 and 3.5. NACA TN 1270, 1947.

4. Anderson, Raymond F.: The Experimental and Calculated Characteristics of 22 Tapered Wings. NACA Rept. 627, 1938.

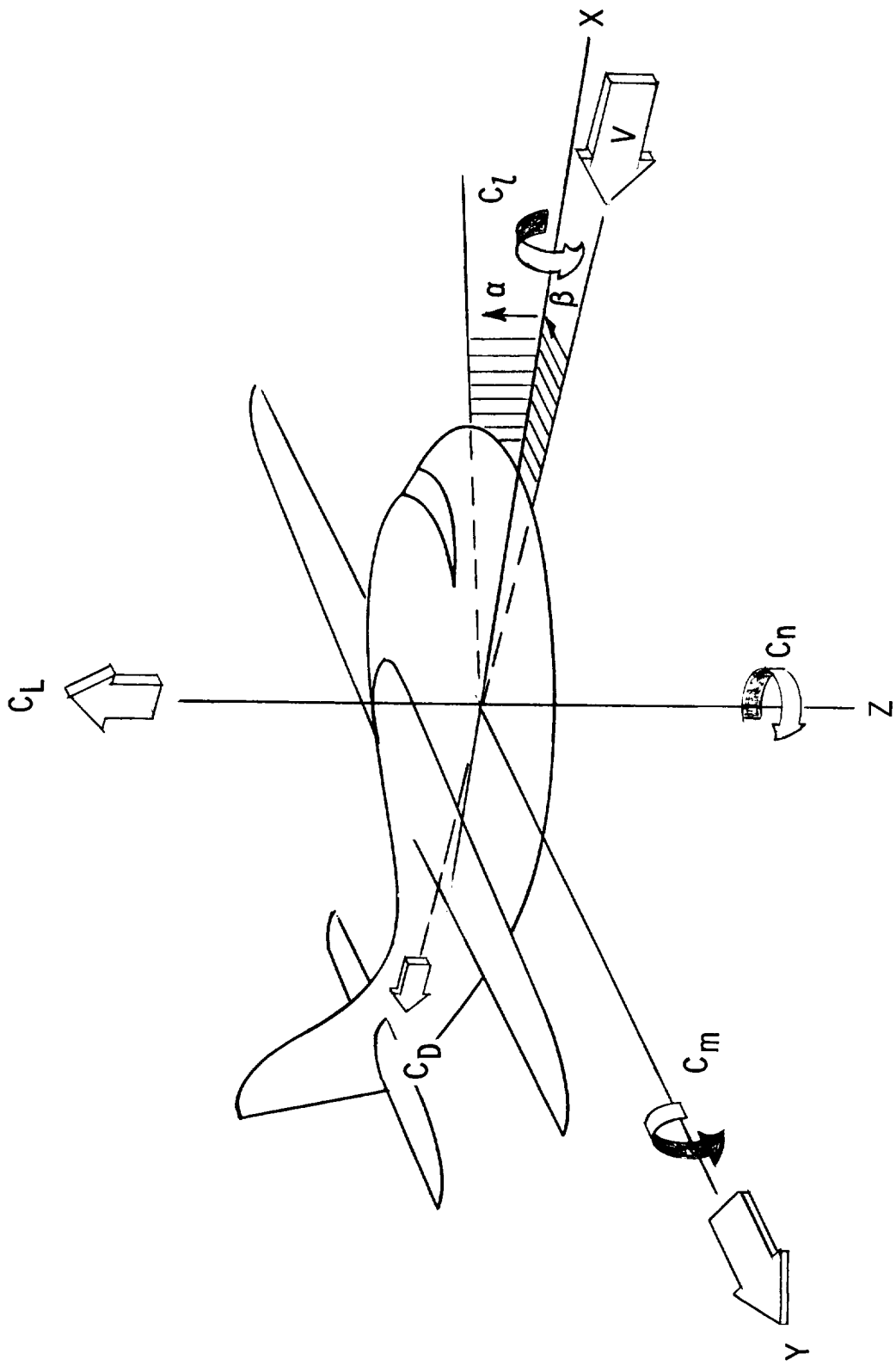

Figure 1.- System of axes and positive sense of angles, forces, and moments.

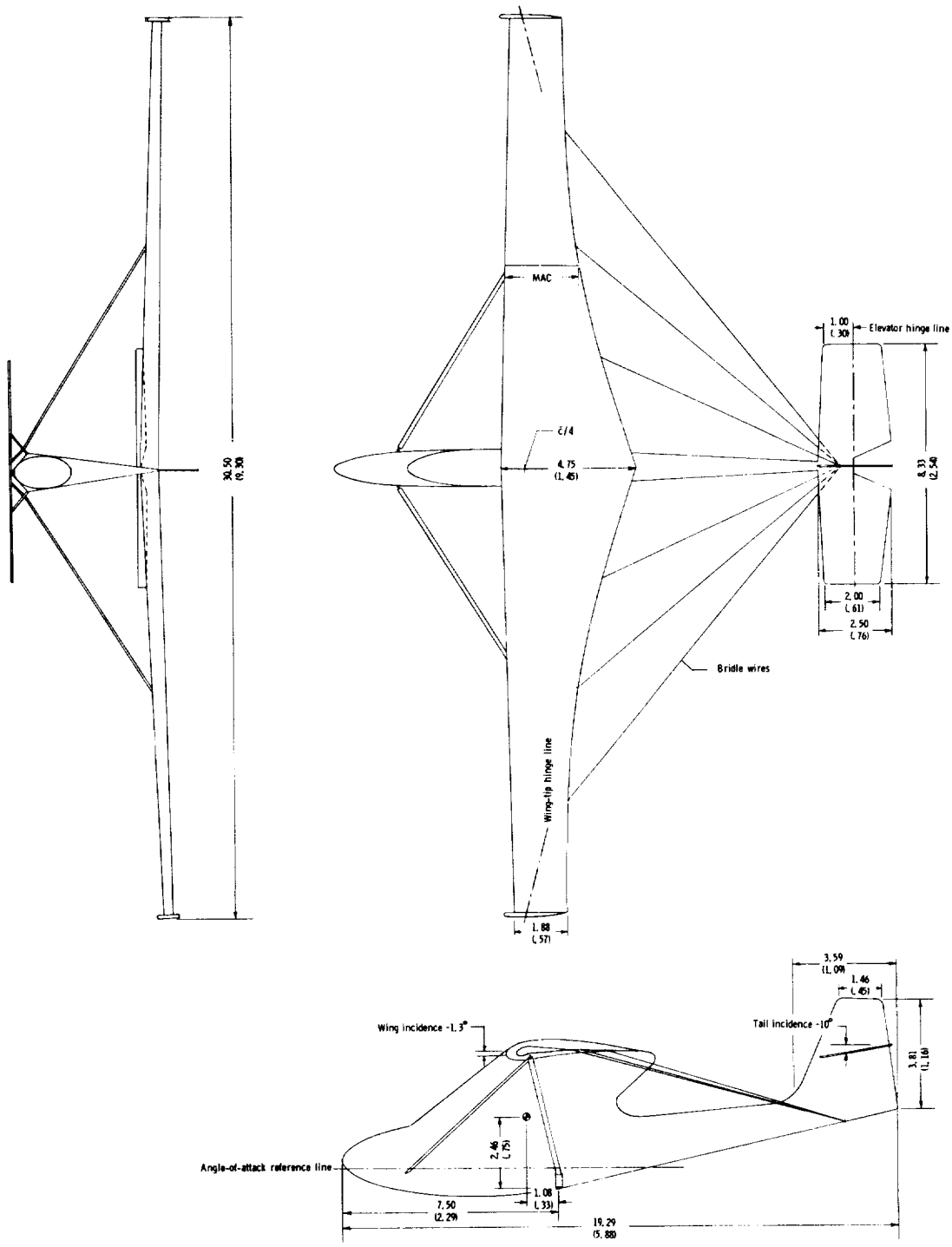

(a) Complete-airplane configuration.

Figure 2.- Drawing of model. Dimensions are given first in feet and parenthetically in meters.

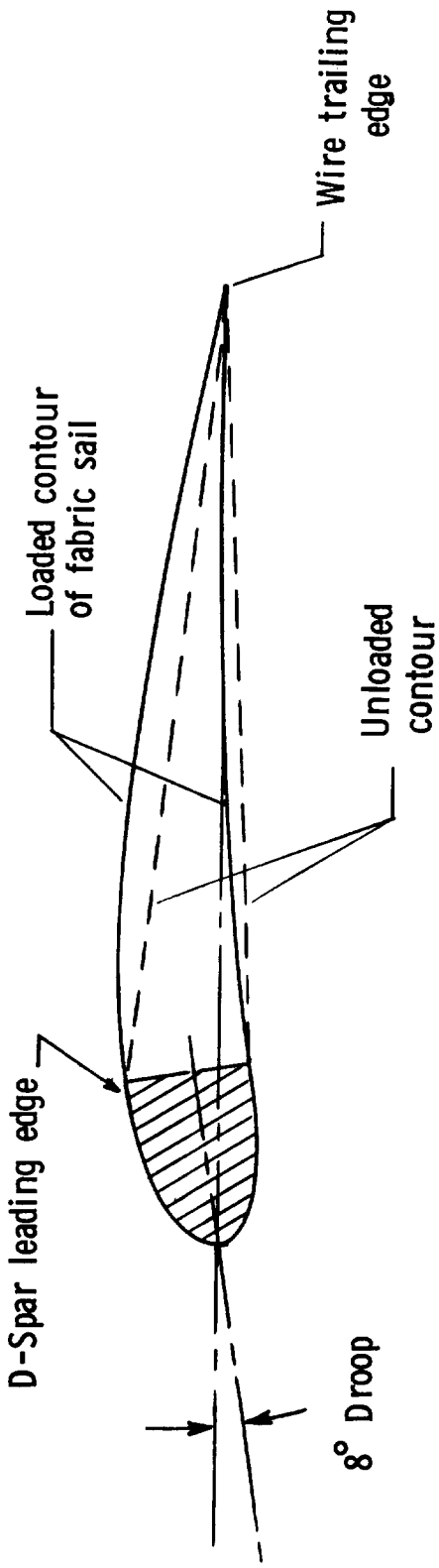

(b) Typical cross section of wing.

Figure 2.- Concluded.

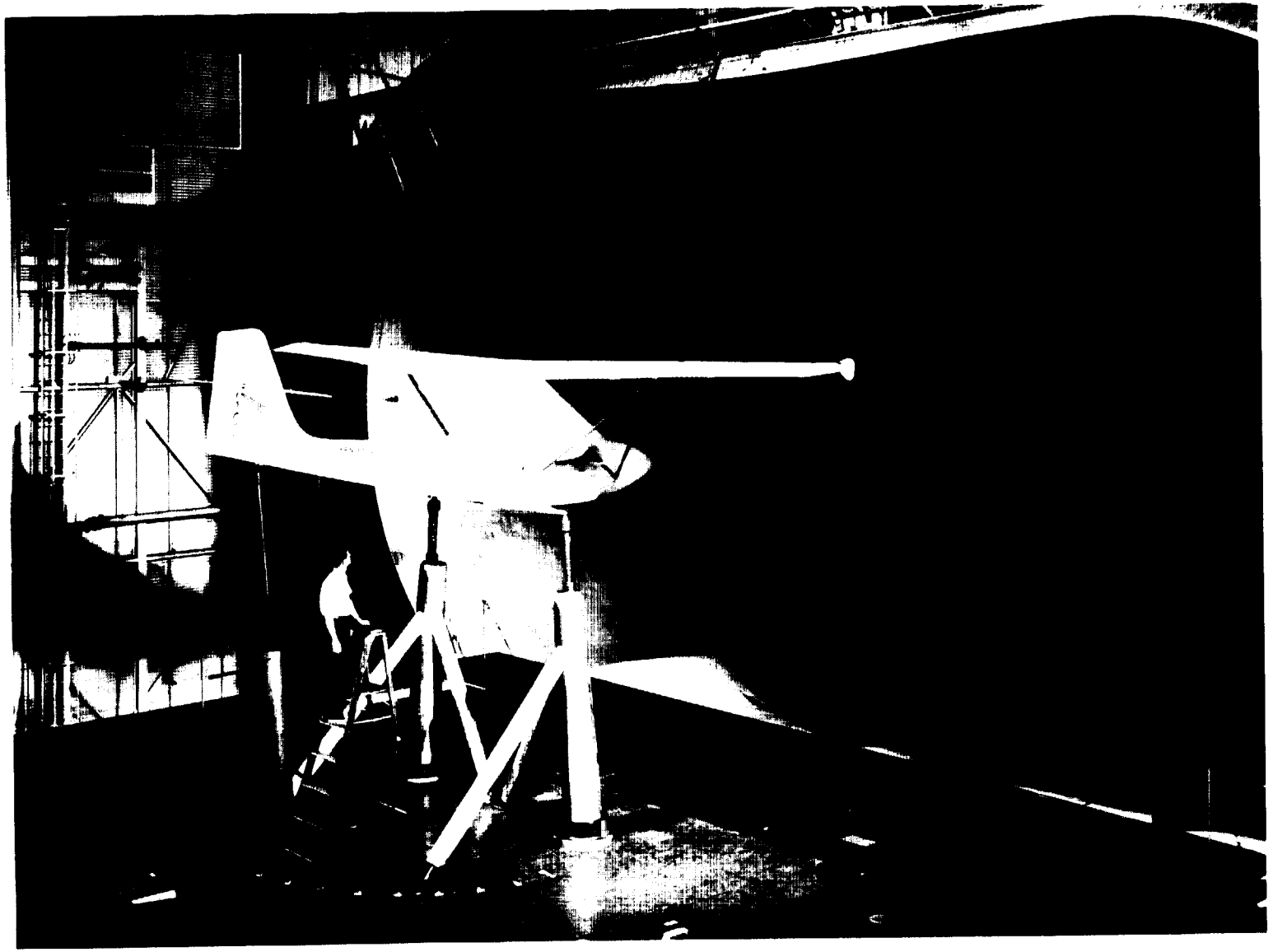

Figure 3.- Photograph of model installed in tunnel.

L-66-4788

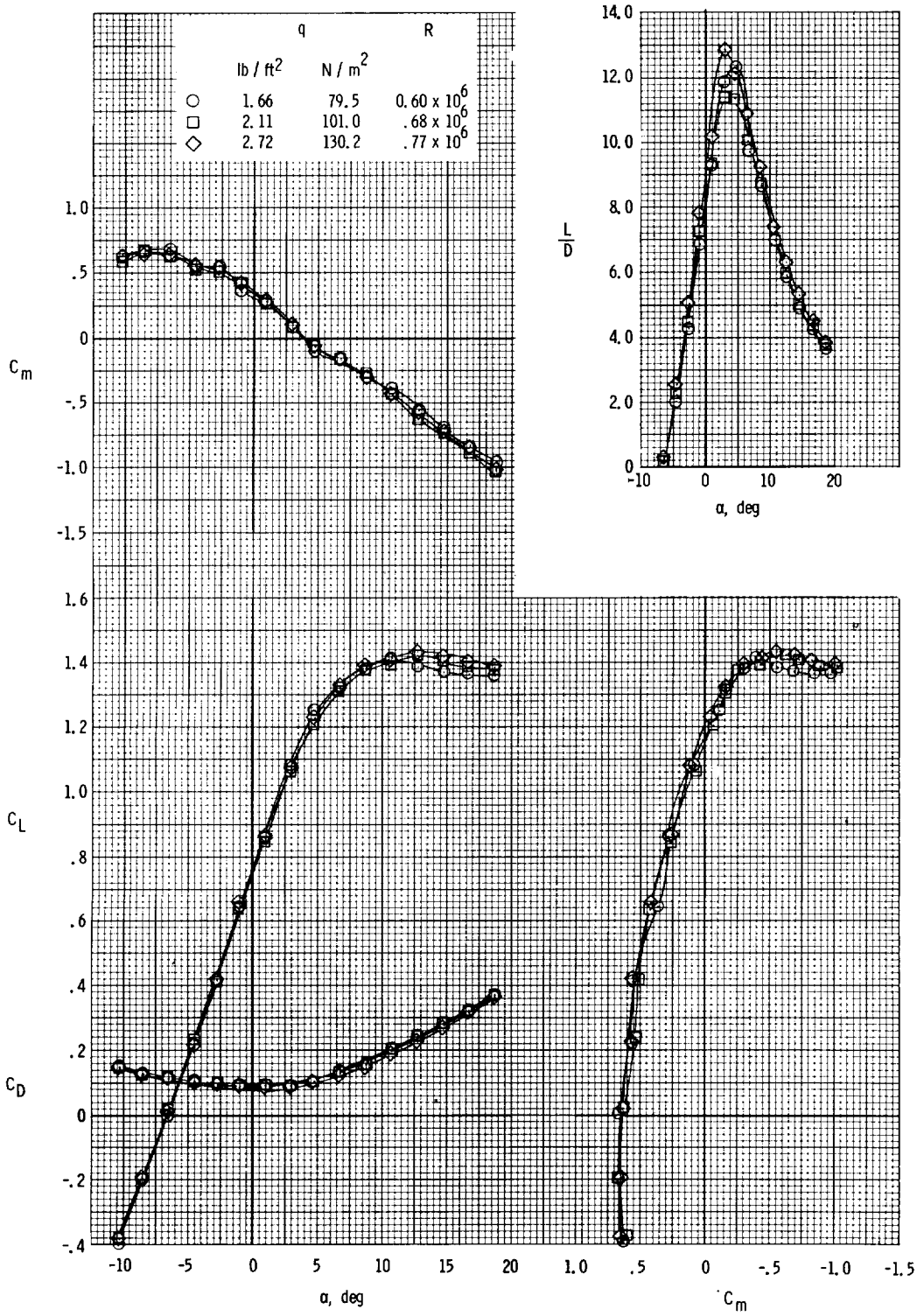

Figure 4.- Effect of dynamic pressure on the longitudinal aerodynamic characteristics of complete model.

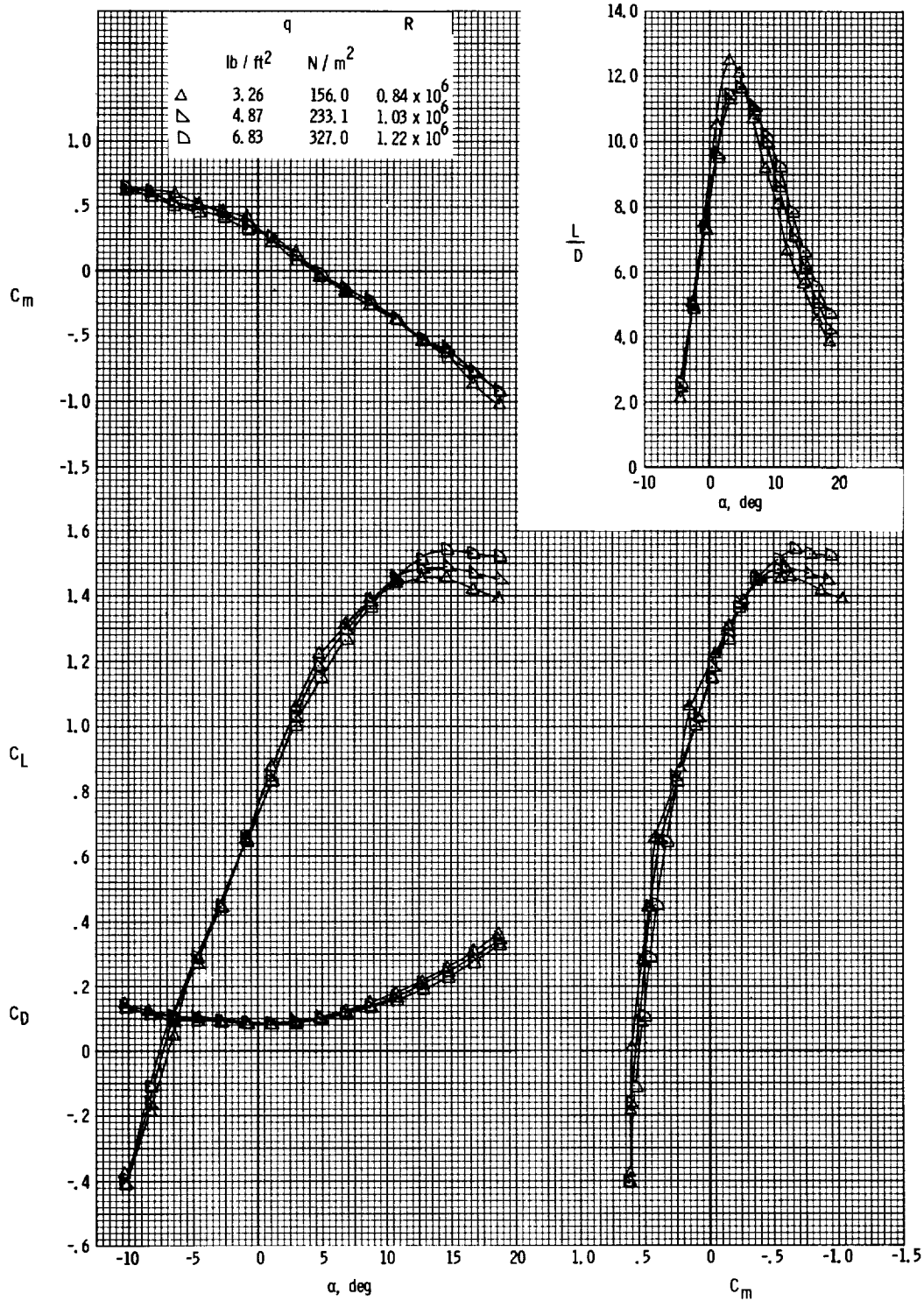

Figure 4.- Concluded.

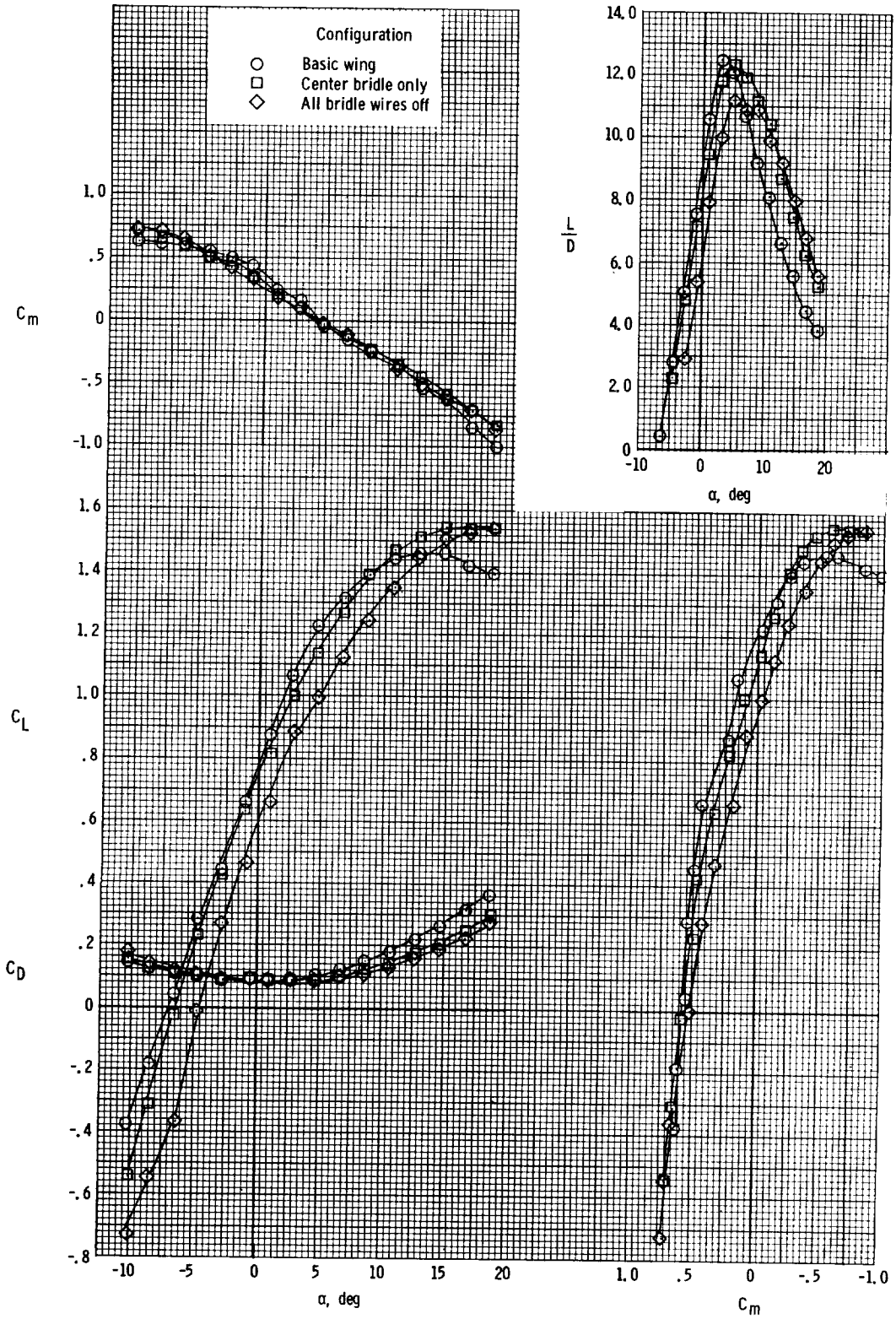

Figure 5.- Effect of bridle wires on the longitudinal aerodynamic characteristics of complete model. $q \approx 3.26$ lb/ft^2 (156.09 N/m^2).

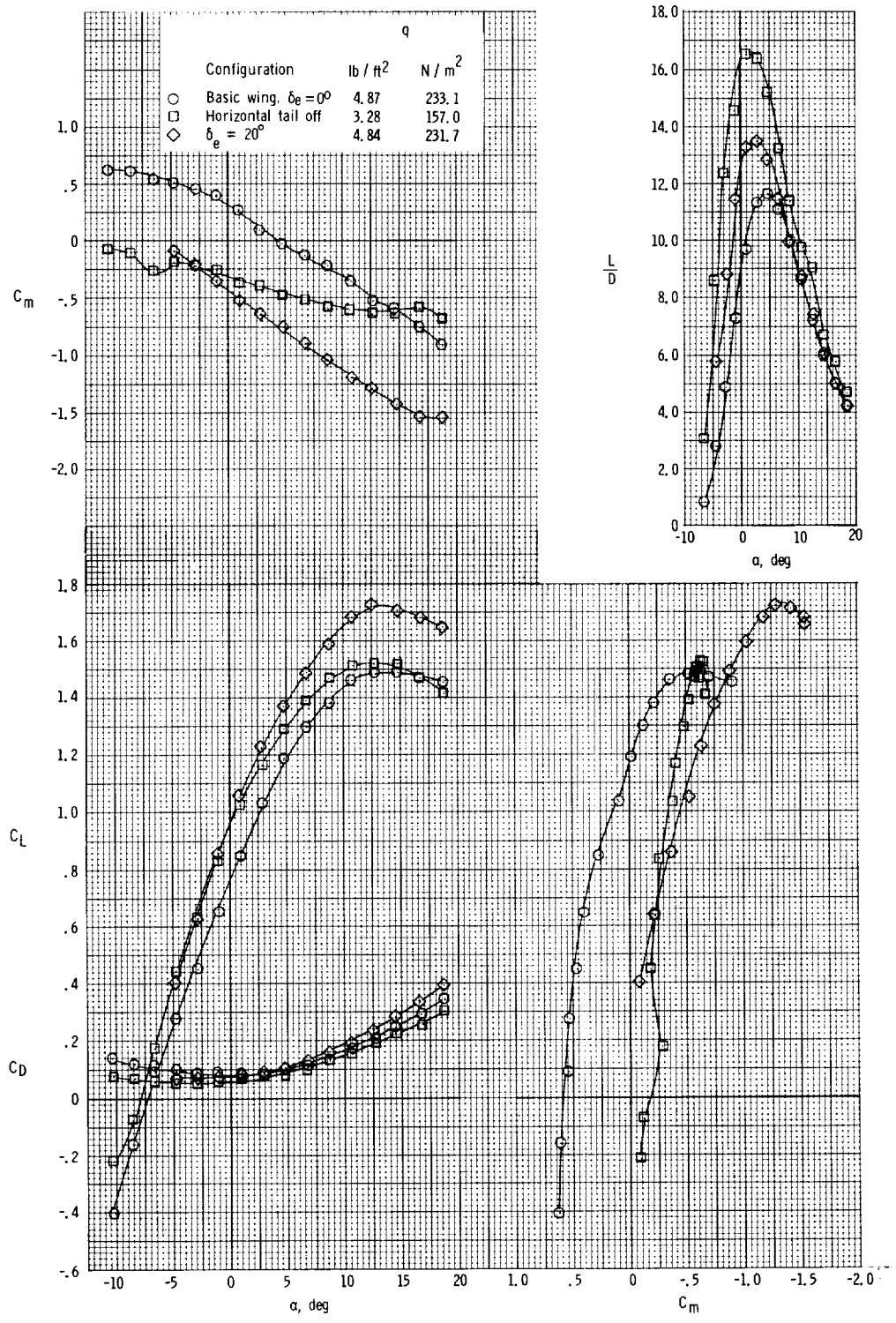

Figure 6.- Effect of elevator deflection on the longitudinal aerodynamic characteristics of complete model.

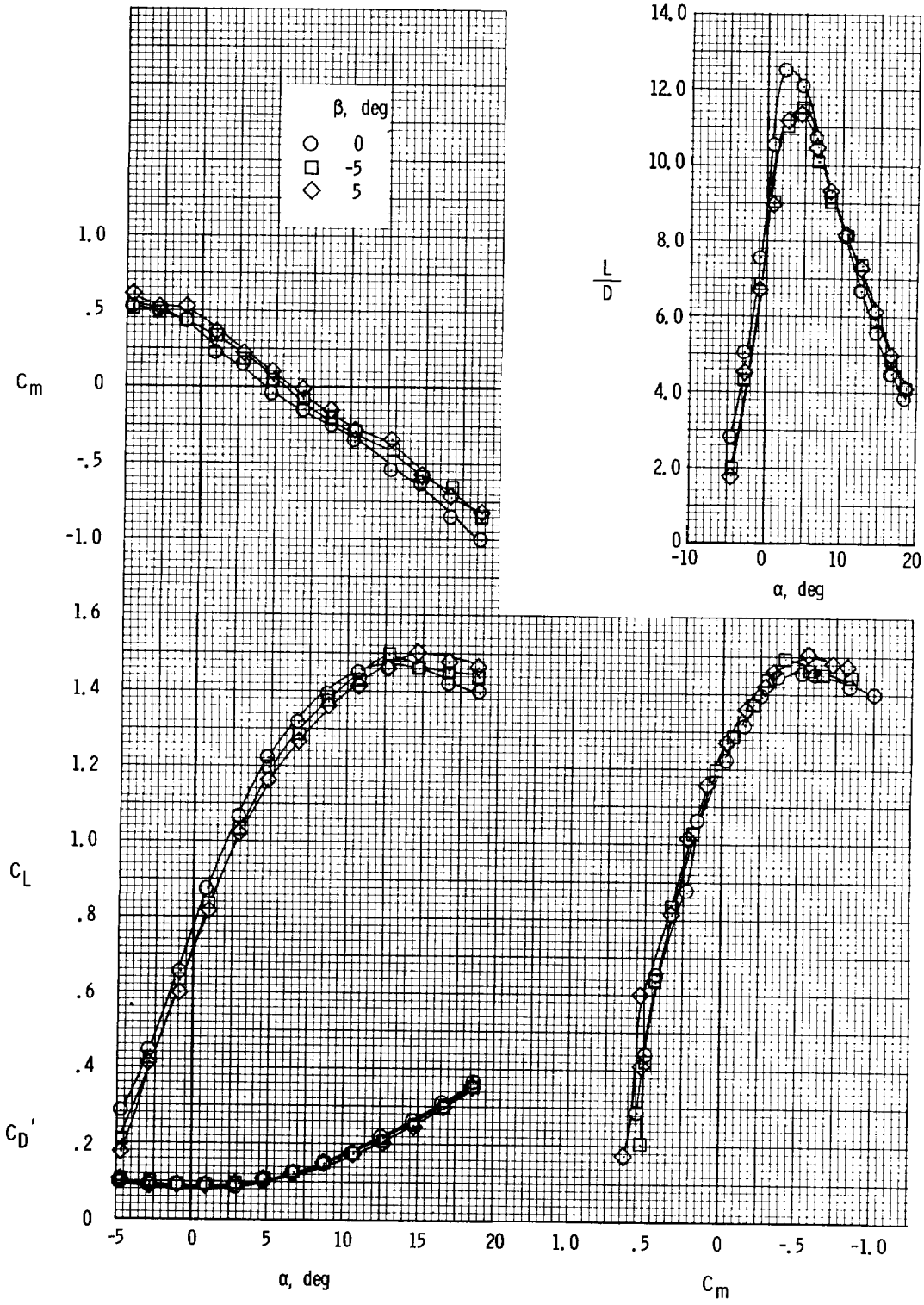

Figure 7.- Effect of sideslip on the longitudinal aerodynamic characteristics of complete model. $q \approx 3.29$ lb/ft^2 (157.53 N/m^2).

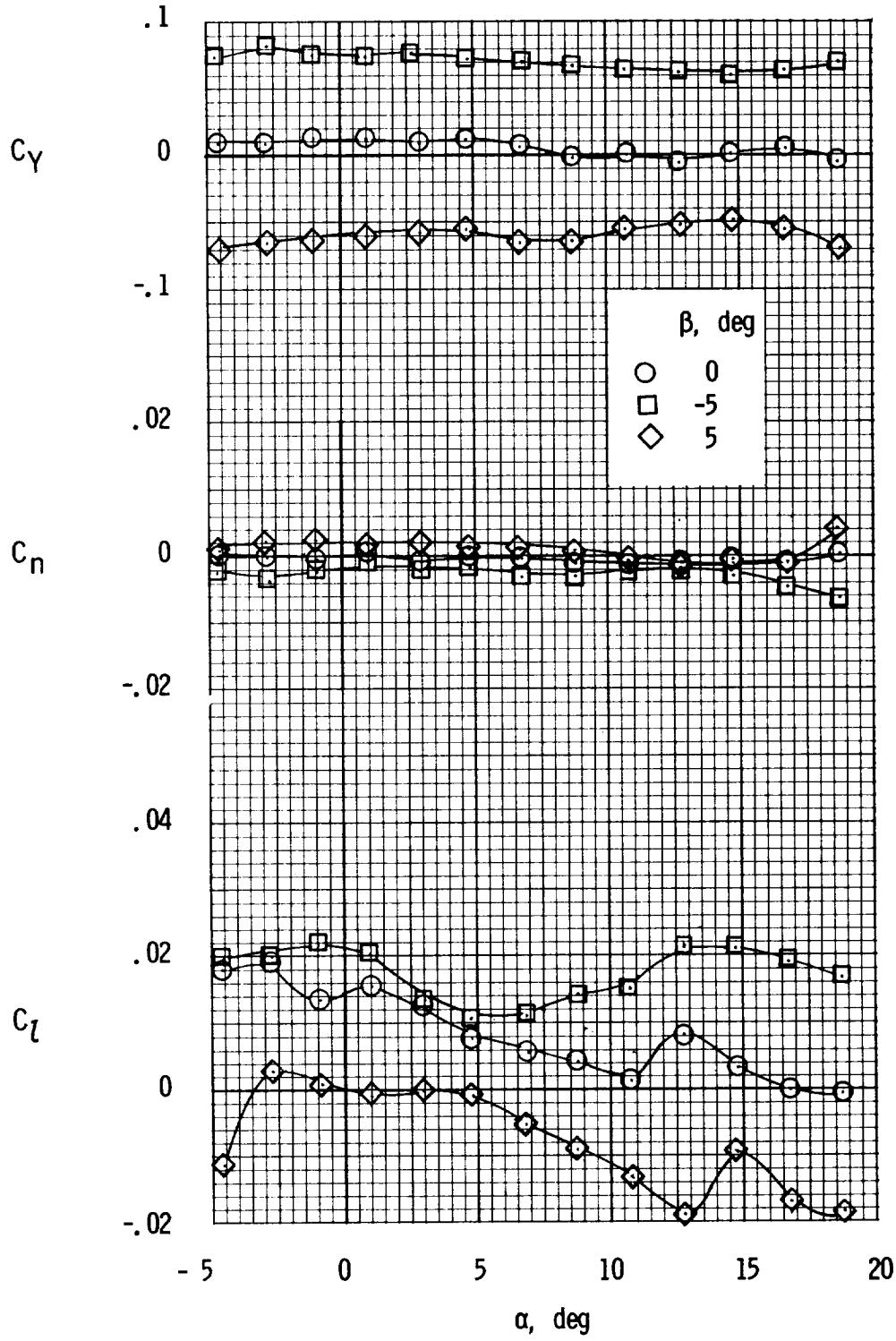

Figure 8.- Lateral stability characteristics of complete model.

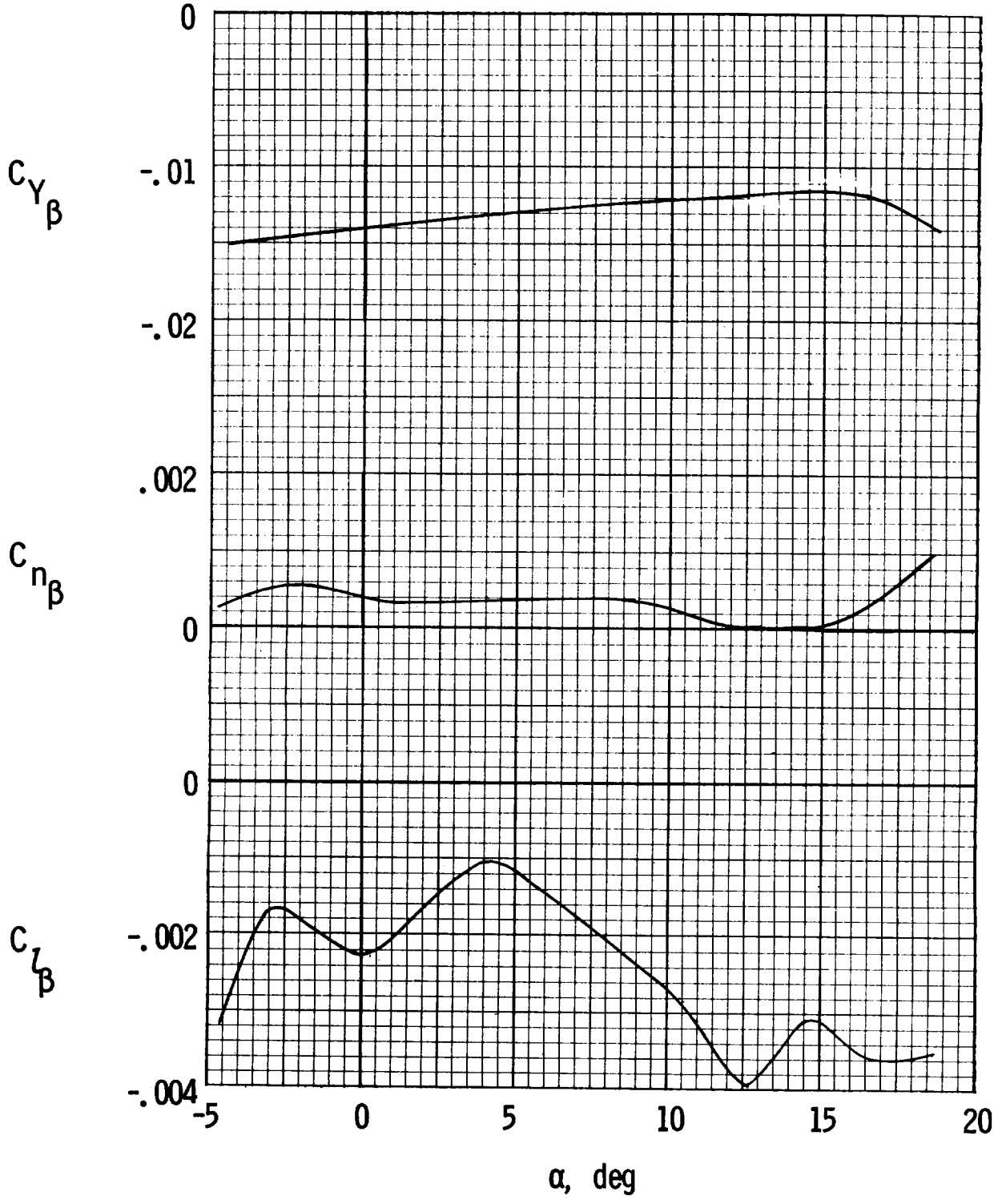

Figure 9.- Variation of lateral-stability parameters with angle of attack for complete model. $\delta_a = 0$.

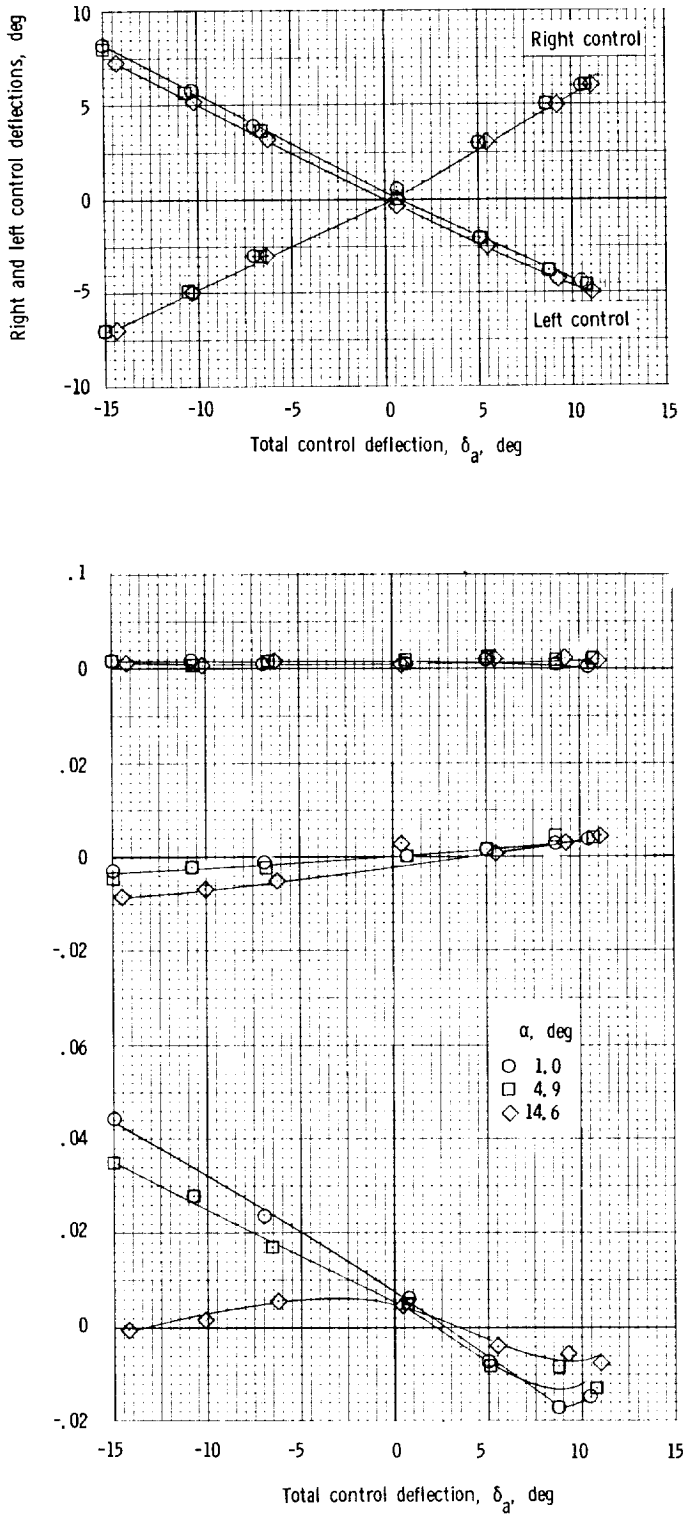

Figure 10.- Lateral control characteristics of complete model at several angles of attack. $q \approx 4.85$ lb/ft^2 (232.22 N/m^2).

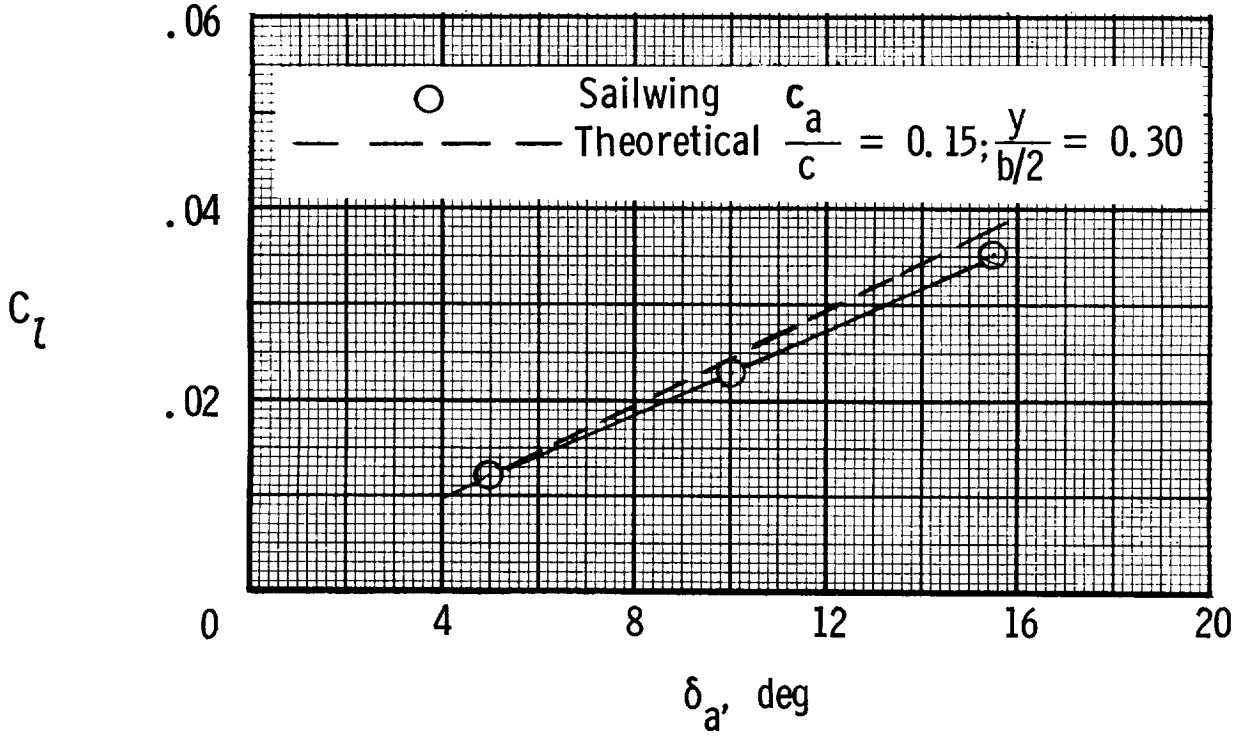

Figure 11.- Comparison of rolling-moment coefficients for the sailwing and a theoretical aileron.

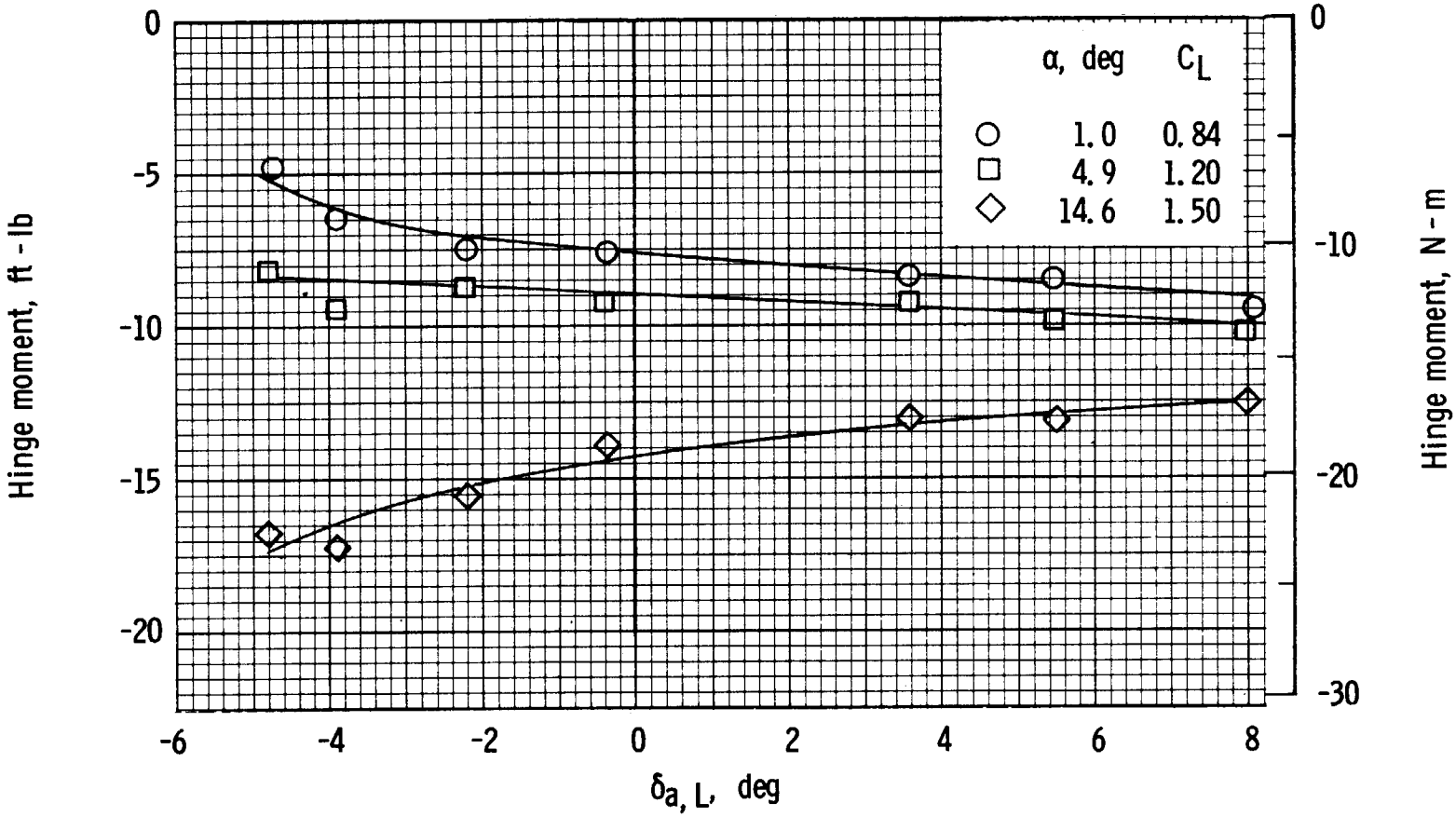

Figure 12.- Variation of hinge moment with control deflection. Trailing-edge-up moments are negative.

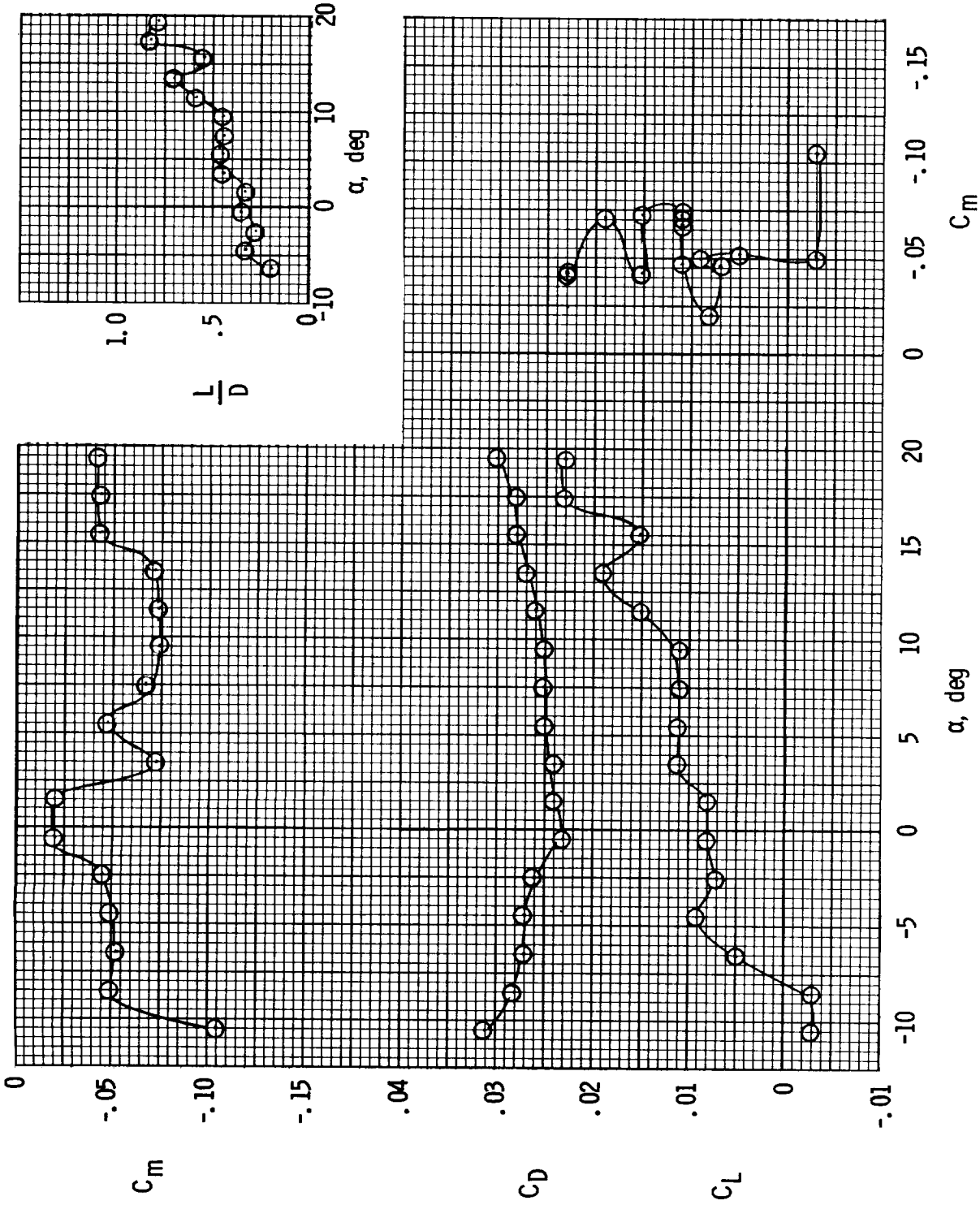

Figure 13.- Longitudinal aerodynamic characteristics of fuselage alone. $q \approx 3.27$ lb/ft^2 (156.57 N/m2).

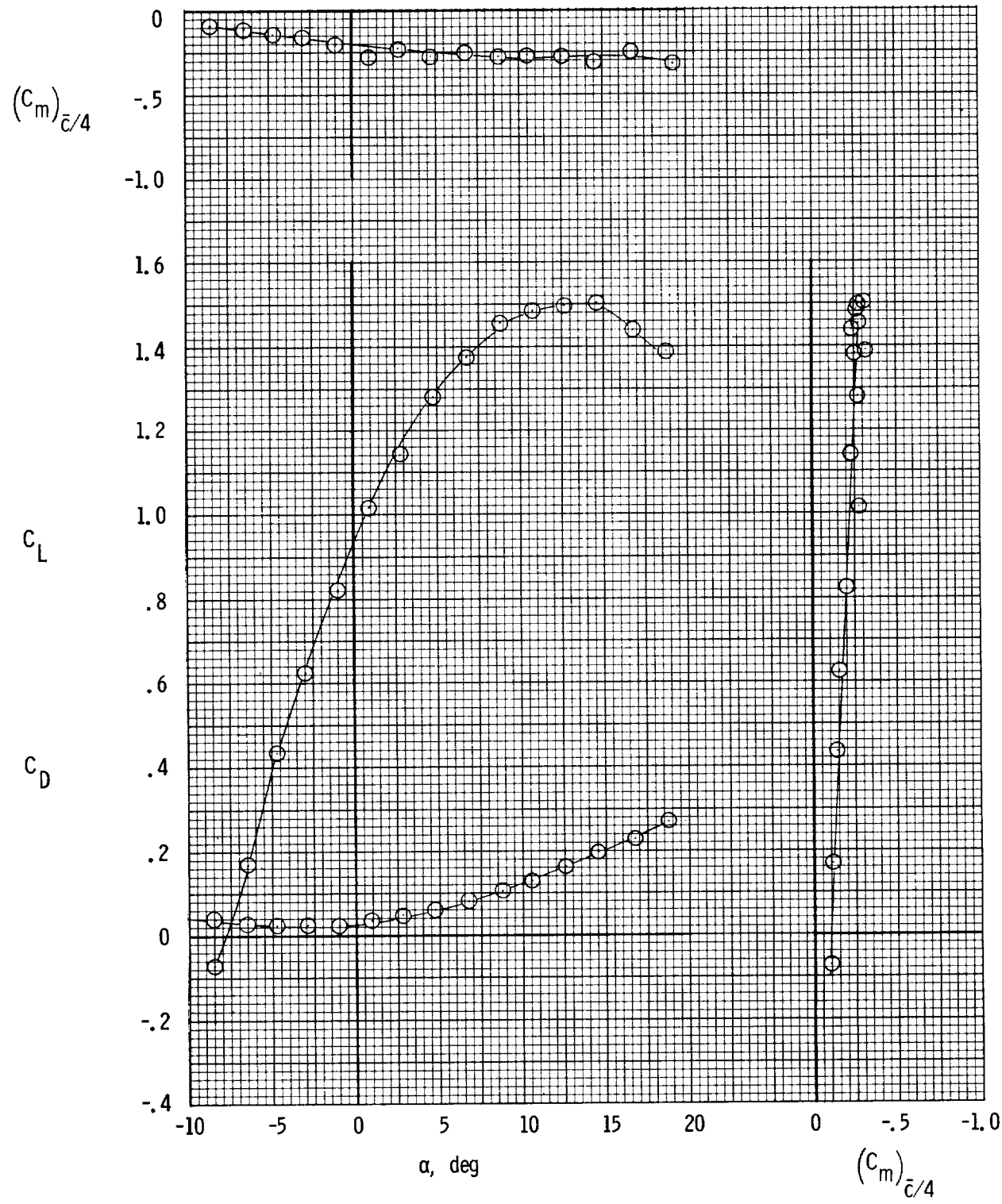

Figure 14.- Aerodynamic characteristics of wing alone. $q \approx 3.27$ lb/ft^2 (156.57 N/m^2).

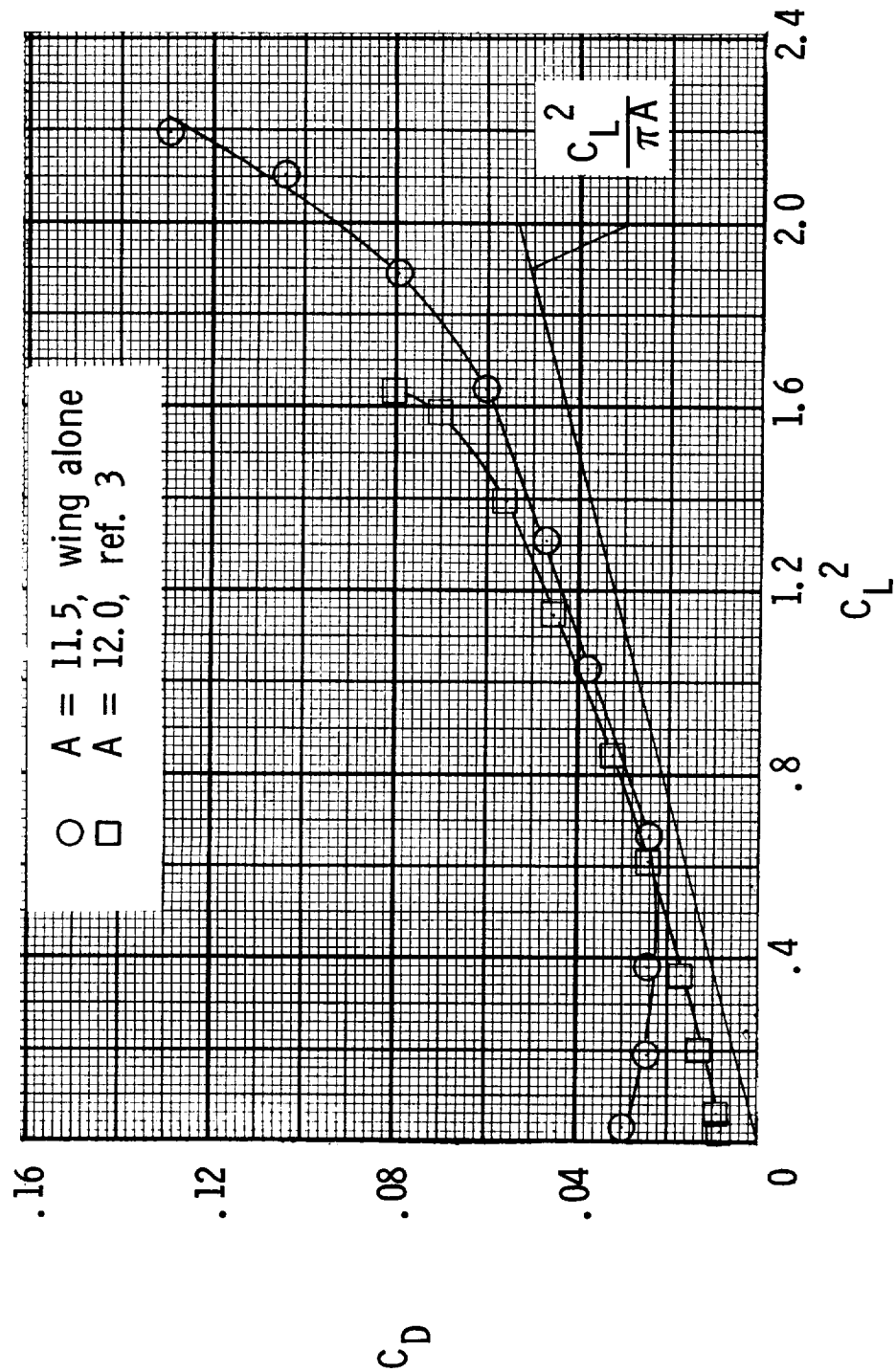

Figure 15.- Comparison of drag characteristics for wing alone and conventional wing.

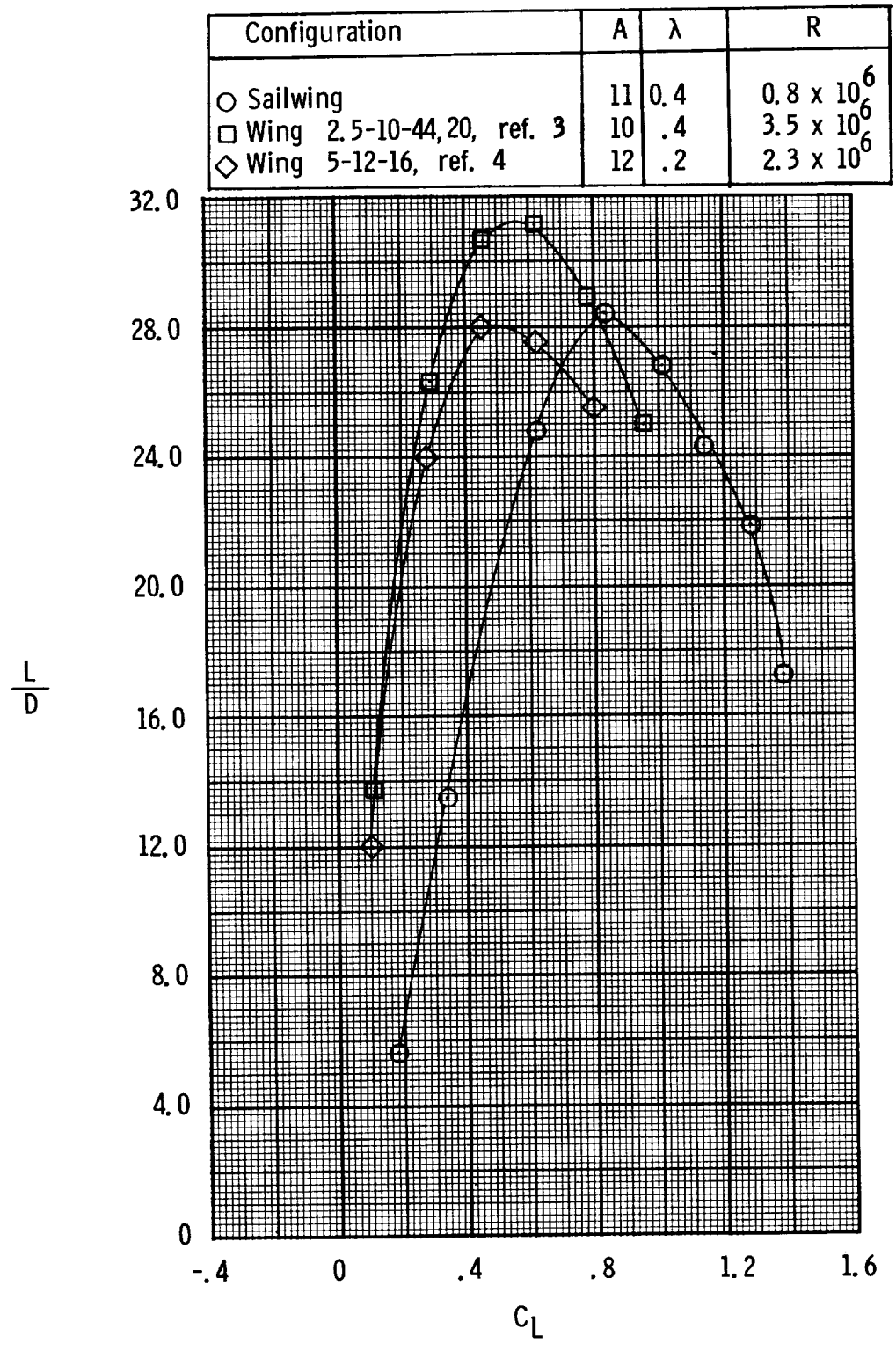

Figure 16.- Comparison of sailwing with conventional wings.

NASA-Langley, 1967 — 1 L-5425

"The aeronautical and space activities of the United States shall be conducted so as to contribute . . . to the expansion of human knowledge of phenomena in the atmosphere and space. The Administration shall provide for the widest practicable and appropriate dissemination of information concerning its activities and the results thereof."

—NATIONAL AERONAUTICS AND SPACE ACT OF 1958

NASA SCIENTIFIC AND TECHNICAL PUBLICATIONS

TECHNICAL REPORTS: Scientific and technical information considered important, complete, and a lasting contribution to existing knowledge.

TECHNICAL NOTES: Information less broad in scope but nevertheless of importance as a contribution to existing knowledge.

TECHNICAL MEMORANDUMS: Information receiving limited distribution because of preliminary data, security classification, or other reasons.

CONTRACTOR REPORTS: Scientific and technical information generated under a NASA contract or grant and considered an important contribution to existing knowledge.

TECHNICAL TRANSLATIONS: Information published in a foreign language considered to merit NASA distribution in English.

SPECIAL PUBLICATIONS: Information derived from or of value to NASA activities. Publications include conference proceedings, monographs, data compilations, handbooks, sourcebooks, and special bibliographies.

TECHNOLOGY UTILIZATION PUBLICATIONS: Information on technology used by NASA that may be of particular interest in commercial and other non-aerospace applications. Publications include Tech Briefs, Technology Utilization Reports and Notes, and Technology Surveys.

Details on the availability of these publications may be obtained from:

SCIENTIFIC AND TECHNICAL INFORMATION DIVISION

NATIONAL AERONAUTICS AND SPACE ADMINISTRATION

Washington, D.C. 20546